



## Acid-base and adsorptive properties of Tunisian Smectite

S. Gammoudi<sup>a</sup>, N. Frini-Srasra<sup>b</sup>, M.A. Goncalves<sup>c</sup>, Ezzedine Srasra<sup>a,\*</sup>

<sup>a</sup>Unité matériaux, Technopole Borj Cedria, BP 95, 2050 Hammam-Lif Tunisie

Email: Srasra.ezzedine@inrst.rnrt.tn.

<sup>b</sup>Faculté des Sciences de tunis, Département de chimie, Université El Manar Tunisie

<sup>c</sup>Faculdade de Ciências da Universidade de Lisboa, Departamento de Geologia and CREMINER/LA-ISR, Edifício C6, Piso 4, 1749–016 Lisboa, Portugal

Received 12 December 2009; Accepted 26 June 2010

### ABSTRACT

Smectite, which is a clay, is a promising material for a large number of applications. This is due to its specific properties i.e. cation exchange and surface complexation on amphoteric edge sites used to describe the uptake of aqueous metal species. This work addresses both properties, firstly by studying the acid-base properties of the Na and Zn-saturated smectites by using both mass and potentiometric titration methods, and secondly by studying Zn(II) adsorption as a function of pH and ionic strength. Mass titration was used to estimate the point of zero proton charge (PZC) by interpolation at different electrolyte concentrations. The potentiometric titration of the two clays suspensions between pH 3 to 11 at varying ionic strengths, 0.5 M, 0.1 M and 0.01 M NaCl was employed to characterize surface charge development on amphoteric edge sites and to graphically determinate the point of zero proton charge (PZC) which were in good agreement with those determined by mass titration. The surface charge formation was similar: positive charges can develop during the protonation reactions of Al-OH sites at edges only at pH values around the pH of PZC and deprotonation of Si-OH and Al-OH sites takes places with increasing pH of the solution resulting in negative charges at the surface edges. The experimental potentiometric data were fitted by applying diffuse double layer model (DDLm) to determine the equilibrium constants of protonation and deprotonation processes using graphic regression, ProtoFit and PHREEQC program. The adsorption of Zn(II) onto a suspension of Na-saturated smectite from Elfahs (Tunisia) was studied as a function of the pH (3, 5 and 7) and ionic strength (0.5 M and 0.01 M NaCl). The adsorption data was then fitted to Freundlich and Langmuir isotherms models.

*Keywords:* Adsorption; Point of zero charge; Clay; Acidity

### 1. Introduction

The presence of heavy metals in the environment, particularly in water and soil is a potential problem because of their high toxicity to plant, animal and human life. Moreover, heavy metals cannot be

destroyed as organic pollutants are. Therefore, several treatment technologies such as chemical precipitation, adsorption and ion exchange using natural, synthetic, modified inorganic and organic solids [1] have been developed for eliminating them from solution. In this group, clay minerals act as potential sorbents for heavy metals thanks to their low cost, specific surface and structural properties, high abundance and easy

\*Corresponding author.

manipulation [2–5]. These clays can sorb heavy metals via two different mechanisms: (1) Cation exchange in the interlayers resulting from the interaction between ions and  $\equiv X^-$  groups of surface sites bearing negative permanent charge and (2) formation of complexes through amphoteric  $\equiv SOH$  groups which can be silanol groups or aluminol groups [6].

The heavy metals of major environmental concern today are copper, nickel, cadmium, lead and zinc. Several studies have been carried out to examine the sorption of zinc by soils and mineral clays. The fixation of  $Zn^{2+}$  by Ca-montmorillonite appears to be controlled by ionic exchange in low ionic strength solution [7]. Na-montmorillonite is a good sorbent of  $Zn^{2+}$  [2]. Cothenbach et al., [8] investigated the potential of montmorillonite, Al-montmorillonite, and gravel sludge to immobilize zinc ions in agricultural soil. The sorption of  $Zn^{2+}$  on Ca-montmorillonite was modeled in terms of cation exchange and surface complexation by [9]. The adsorption of  $Zn^{2+}$  on kaolinite is proposed to involve the formation of bidentate surface complexes [10]. Modified clay sorbents exhibit much higher adsorption capacity for zinc ions than that of natural clays [11]. Sorption of zinc ions by six mixed mineral systems was studied by [12]. Limed-treated montmorillonite is used to adsorb  $Zn^{2+}$  in a wide range of  $Zn^{2+}$  concentrations [13]. The majority of studies have demonstrated the influence of several factors in the Zn(II) adsorption such as pH [4,5,14] and ionic strength [7,12]. However, in spite of this large amount of work, few studies characterised acid-base behaviour of adsorbent and its interaction with  $Zn^{2+}$  [15,16,17].

The aim of the present work is (1) to study the interaction between a Na-saturated Tunisian smectite and  $Zn^{2+}$  in aqueous solution to determine the effects of pH and ionic strength (2) to characterize the acid-base behaviour of Na-smectite and Zn-smectite, interpreted in terms of the Non-Electrostatic Model (NEM).

## 2. Methods and materials

The sample clay used in this study came from Elfahs (North-east Tunisia). This clay was purified using the classical method of [18]. To obtain the monocationic Na-clay (Na-EP) it was treated with 1 M NaCl. The suspension was then centrifuged 2700 rpm, and the supernatant solution was discarded and replaced with fresh solution. The procedure was repeated five times. The Na-clay was then washed/dialysed in deionised water until excess  $Cl^-$  was totally eliminated (undetected by the  $AgNO_3$ ). The clay exchanged by zinc (Zn-EP) was obtained using the same procedure.

### 2.1. Physical and chemical characterization

#### 2.1.1. X-ray diffraction

X-ray diffraction patterns were recorded using a “PANalytical X’Pert HighScore” diffractometer with  $\alpha_1$  of copper radiation. Two types of diffractograms were studied: diffractograms with disorientated powder where all the (h k l) peaks appear and diffractograms of plate oriented obtained by sedimentation. This makes it possible to determine the stacking periodicity of the layers, with the identification based on the ( $d_{001}$ ) reflection.

#### 2.1.2. Chemical composition and structural formula

The clay sample was attacked by a mixture of three acids (HCl,  $H_2SO_4$ , and  $HNO_3$ ). All the elements passed into solution, except the silica ( $SiO_2$ ) which is determined by gravimetry. The other elements, such as Al, Fe, Mg, Ca, Na and K were assayed by Atomic Absorption Spectrophotometer (AAS).

#### 2.1.3. Cation exchange capacity (CEC) and specific surface area (SSA)

CEC was determined by the method of copper ethylenediamine ( $EDA$ ) $_2CuCl_2$  complex [19]. SSA was determined by nitrogen gas adsorption at 77 K, using a “Quantachrom-Autosorb1” sorptimeter.

### 2.2. Surface acidity

#### 2.2.1. Mass titration

According to the method described in the literature [20,21], our experiments on mass titrations were performed. Approximately 0.05 g of dry Na-EP or Zn-EP was added to 50 ml of a NaCl solution at different ionic strengths (0.5 M and 0.1 M) and different pH values (4, 5, 8 and 10). After each addition, the pH was recorded after an “equilibrium time” of about 10 min. Then, a new amount of sample was introduced which induced a change in the solution pH. This procedure was repeated until the pH was found stable after the addition of the sample. This was the pH where proton adsorption was zero (PZC).

#### 2.2.2. Potentiometric titration

The pH-dependent surface charge was determined by potentiometric acid-base titration using NaCl as background electrolyte at constant ionic strengths of 0.5 M, 0.1 M and 0.01 M. The pH was measured using the pH-meter corning pH glass combination electrode which was calibrated with buffer solutions (pH = 4, pH = 9.18).

For all the acid-base titrations, 0.1 g of Na-EP or Zn-EP was added to a 15 ml water flask and stirred for 24 h. Suspensions were acidified by the addition of 0.001 M HCl to adjust the pH value of the suspension to approximately 3. Distilled water was added to bring the total initial volume of the suspension to 30 ml. The samples were stirred for 20 min. Then, 0.05 ml increments of 0.05 M NaOH were used to titrate the suspensions up to a pH of approximately 11. During the titration period, the mixture was stirred with a magnetic stirring bar and the temperature was held constant at 298 K.

### 2.3. Adsorption isotherms

An amount of 100 mg of Na-smectites Na-EP with different volumes of 0.01 M zinc mother solution was placed in polypropylene tubes at the beginning of the experiments. The metal ion concentration used in the tests ranged between 15 mg·l<sup>-1</sup> to 200 mg·l<sup>-1</sup>. The ionic strength was varied between 0.01 M and 0.5 M using NaCl as background electrolyte. The batch adsorption experiments were also conducted at different pH values (3–7) adjusted by adding diluted NaOH and/or HCl solutions. The solution pH was adjusted before adding the clay because bentonites tend to increase the solution pH after being added into solution. The agitation speed was constant and kept at 2700 rpm during the test at 298 K. The experiments were terminated after a contact time of 6 h. At the end of each run, the sample was centrifuged and the supernatant liquid was analysed for Zn by Atomic Absorption Spectrophotometer. The amount of metal adsorbed was estimated by the difference between the initial concentration in the solution and the concentration after equilibrium had been reached. Adsorption isotherm data were fitted to Langmuir and Freundlich equilibrium equations.

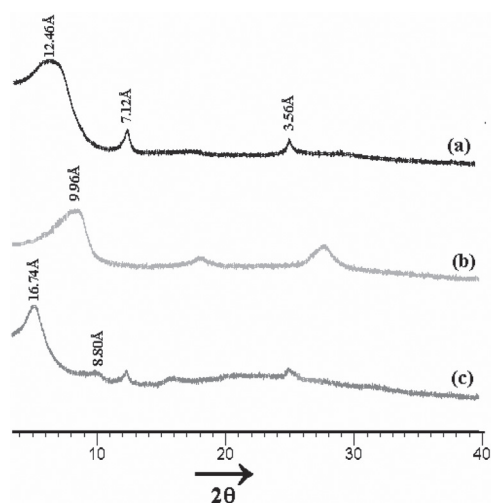


Fig. 1. XRD diffractograms of Na-EP, (a) purified clay; (b) heated at 550 °C; (c) treated by ethylene glycol.

## 3. Results and discussion

### 3.1. Physical and chemical characterization

Fig. 1 shows the diffractograms of purified clay Na-EP. The  $d_{001}$  reflection appears at 12.46 Å indicating the presence of Na-smectite. After treatment by ethylene glycol the peak moved to 16.74 Å. Moreover, the  $d_{002}$  appearing at 8.80 Å reveals that Na-EP is an interstratified illite-smectite. The percentage of smectitic fraction is estimated to be 78%. Also, the  $d_{001} = 7.12$  Å and  $d_{002} = 3.56$  Å indicate the presence of a small amount of kaolinite, which disappear after heating at 823 K.

Fig. 2 shows the diffractograms of the clay Zn-EP, we observe again the presence of smectite ( $d_{001} = 14.83$  Å). The difference in the position of the main (001) peak for Na-EP and Zn-EP drawn by the cation-exchange processes: amount of the cation inserted in side the inter-layer of smectite [20]. Also for Zn-EP, the  $d_{001}$  passed to 16.4 Å and to 9.7 Å after treatment by ethylene glycol and after heating at 823 K.

The structural formulas of exchanged purified clays Na-EP and Zn-EP were  $(\text{Si}_{7.86}\text{Al}_{0.14})(\text{Al}_{2.98}\text{Fe}_{0.39}\text{Mg}_{0.65})\text{Ca}_{0.06}\text{Na}_{0.44}\text{k}_{0.12}\cdot\text{O}_{20}(\text{OH})_4$  and  $(\text{Si}_{7.86}\text{Al}_{0.14})(\text{Al}_{2.98}\text{Fe}_{0.39}\text{Mg}_{0.65})\text{Zn}_{0.23}\text{Ca}_{0.03}\text{Na}_{0.04}\text{k}_{0.12}\cdot\text{O}_{20}(\text{OH})_4$ , respectively. The CEC are 77.3 and 77.5 meq/100 g; the  $S_{\text{BET}}$  are 92.74 and 116.5 m<sup>2</sup>·g<sup>-1</sup> for Na-EP and Zn-EP respectively.

### 3.2. Surface acidity

#### 3.2.1. Mass titration

Mass titration data performed on the Na-EP and Zn-EP at 0.5 M and 0.1 M NaCl are presented in Fig. 3. The pH gradually changes with addition of solid mineral and asymptotically approaches a limiting value.

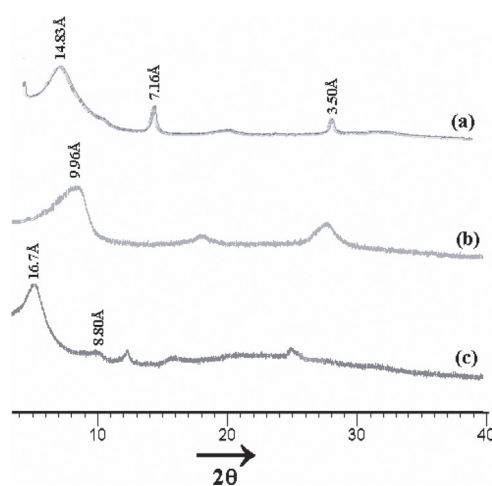


Fig. 2. XRD diffractograms of Zn-EP, (a) purified clay; (b) heated at 550 °C; (c) treated by ethylene glycol.

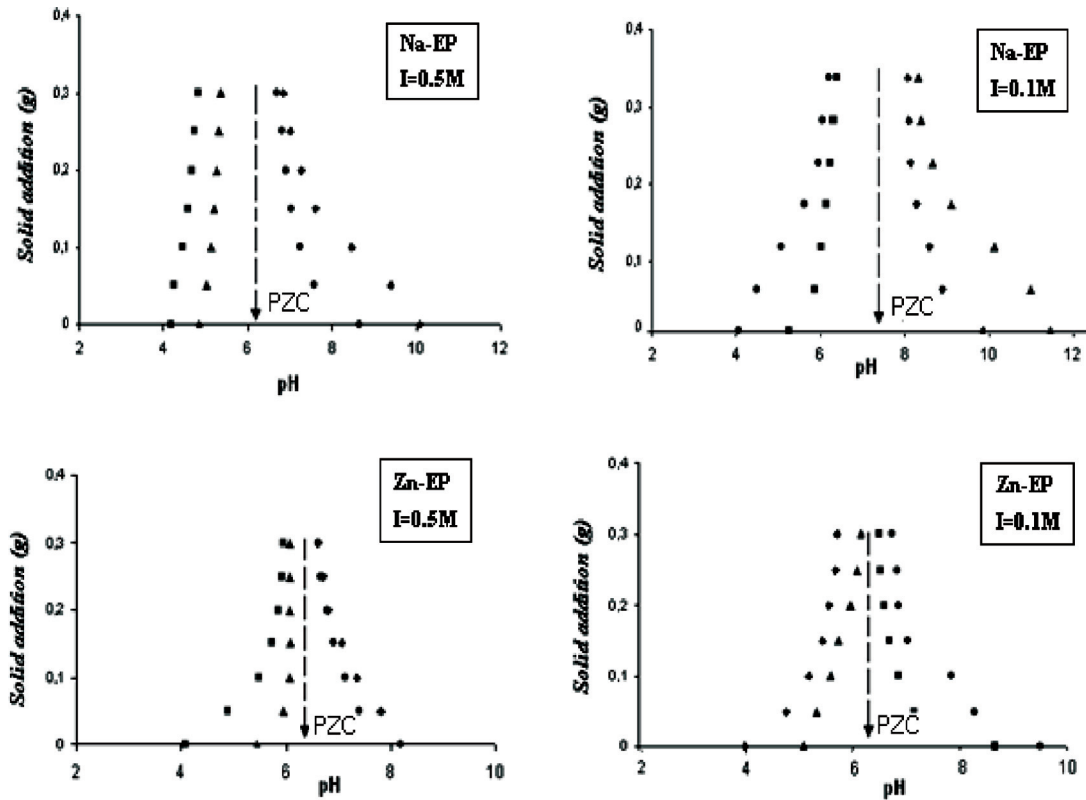


Fig. 3. Mass titration of Na-EP and Zn-EP obtained at 0.5 M and 0.1 M. Each solid addition corresponds to 0.05 g of two samples at different pH.

The direction of pH variation depends on the pH of the starting NaCl solutions. Therefore, the pH where solid addition does not produce any change in the pH of the initial NaCl solution can be estimated by interpolation. The values of PZC estimated for two clays are reported in Table 1 for the titration performed at 0.5 M and 0.1 M NaCl.

3.2.2. Potentiometric titration

All potentiometric titration curves of Na-EP and Zn-EP were performed at different ionic strengths and in the pH range from 3 to 11 in order to measure the surface proton density (the proton adsorption)  $\sigma_H$  which was calculated as the difference between the total amount of  $H^+$  or  $OH^-$  added to the dispersion and that

required to bring a blank solution with the same NaCl concentration at the same pH [21]:

$$\sigma_H \text{ (mol}\cdot\text{m}^{-2}\text{)} = \frac{V}{m} S \left\{ \left( \left[ H^+ \right]_b - \left[ H^+ \right]_s \right) - \left( \frac{K_w}{\left[ H^+ \right]_b} - \frac{K_w}{\left[ H^+ \right]_s} \right) \right\} \quad (1)$$

where  $V$  is the electrolyte solution volume equilibrated with the clay mineral (ml);  $[H^+]$  is the solution proton concentration;  $K_w$  is the dissociation product of water; subscripts “s” and “b” refer to sample and blank solution;  $m$  is the mass of sample used (g) and  $S$  is the specific surface area ( $\text{m}^2\cdot\text{g}^{-1}$ ).

The experimental data surface proton density  $\sigma_H$  versus pH function of the purified Na-EP and Zn-EP dispersed in 0.5 M, 0.1 M and 0.01 M NaCl concentration are shown in Fig. 4. The behaviour of our titration curves are similar in shape for the pH range used and are reproducible when compared to those published in the literature [22,23]. As it can be seen, two branches of the titration curves were obtained:  $\sigma_H$  is positive in

Table 1  
PZCs determined from mass titration curves of Na-EP and Zn-EP

Sample	Ionic strength	
	0.5 M	0.1 M
Na-EP	6.39	7.26
Zn-EP	6.08	6.28

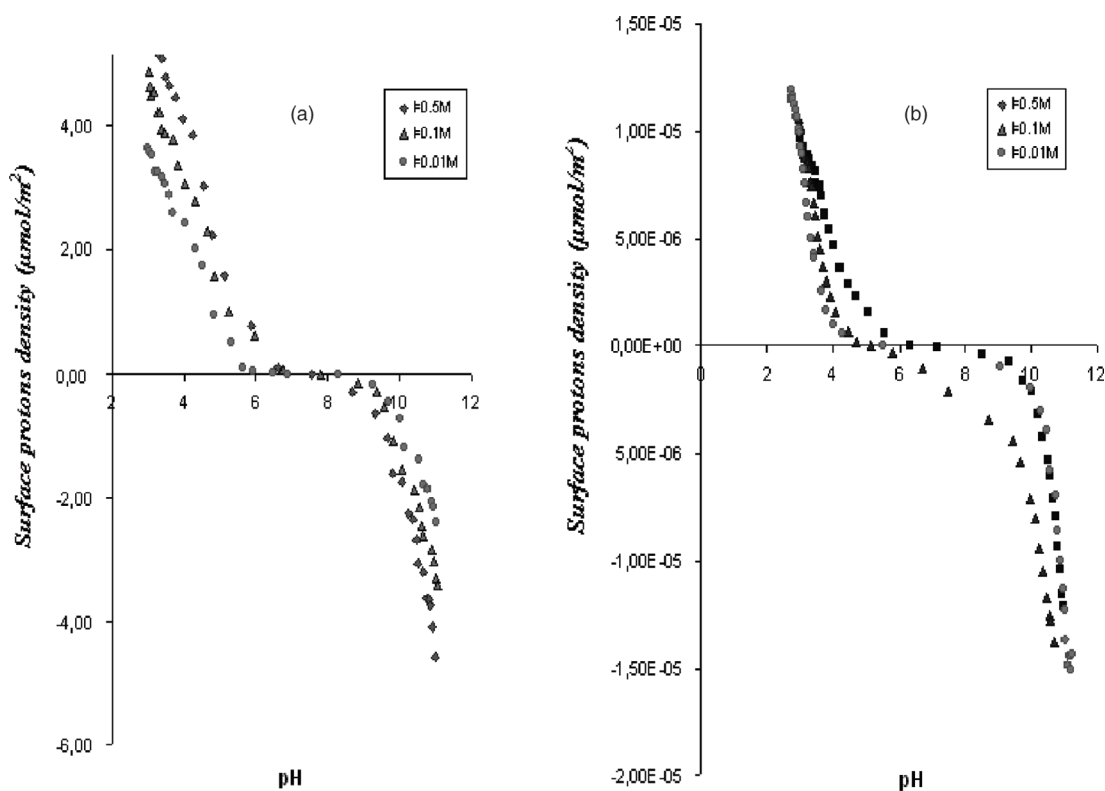


Fig. 4. Potentiometric titration curves versus pH at different ionic strengths, at 298 K: (a) Na-EP, (b) Zn-EP.

acidic pH range due to the protonation of surface functional groups and negative in the alkaline range due to deprotonation. Tombáč and Szekeres [24] suggest that the positive charge is developed only on the Al-OH sites at the surface edges of 2:1 or 1:1 clays at pHs below the pH where  $\sigma_H > 0$  and deprotonation occurs on both Si-OH and Al-OH sites with increasing pHs resulting in negative charges at surface edges similar to those on flat faces.

The potentiometric titration curves of two samples at different electrolyte concentration (0.5, 0.1 and 0.01 M NaCl) reveal that, for acidic pH range, the degree of protonation increases with increasing ionic strength and the opposite is true for the alkaline pH range. This dependence of the density surface charge on the ionic strength is due to the fact that ionic strength had significant and contrasted effects on the dissolved species Al, Si, Fe and Mg [25]. Therefore, the most striking observation in Fig. 4 is the absence of the expected common intersection point, assigned as the point of zero salt effect PZSe [26]. It is evident from Fig. 4 that the PZCs of the two samples; depends on the ionic strength. The values for the two clays are given in Table 2. Our results show that purified Zn<sup>2+</sup>-smectite has a PZC value lower than purified Na<sup>+</sup>-smectite.

Table 2  
PZCs determined by potentiometric titration curves of Na-EP and Zn-EP

Sample	PZC
Na-EP	6.4–7.8
Zn-EP	5.8–7.2

In comparison with the mass titration method, the values agree for the Zn-EP sample but fall short of the lower limit of the potentiometric titration for the Na-EP. Although not easily explained, each method may develop quite different equilibrium conditions with the clay suspension that may in turn show these discrepancies.

### 3.2.3. Modelling acid-base

In studies of the surface acid-base behaviours of aqueous montmorillonite [6,24,25], a weakly acidic surface functional group ( $\equiv\text{XH}$ ) accounting for ion exchange reactions was incorporated along with the amphoteric surface hydroxyl group ( $\equiv\text{SOH}$ ) into the surface protonation model. In our work, since we used very high background electrolyte concentration ( $>10 \text{ mmol}\cdot\text{l}^{-1}$ ), we only considered the acid-base behaviour of the

amphoteric surface hydroxyl groups ( $\equiv\text{SOH}$ ) in simulating the surface reaction of the two clays. Therefore, to evaluate the potentiometric data measured by acid-base titration at different ionic strength allows us to calculate the density surface charge of amphoteric edge sites; we choose a simple model approach using the principals of Non-Electrostatic Model (NEM). Our approach was similar to the simple model developed by [22,27], since we know that our potentiometric titration curves are similar to those obtained by the same authors. It is based on simple adsorption isotherms in which it simulates protonation and deprotonation reactions. This model assumes that the system can be described by a simple mass action law, where the activity coefficients of the surface species remain constant during the experiment. We assumed that there are mainly two kinds of surface sites: a protonation site and a deprotonation site.

The protonation and deprotonation reactions of two sites are represented by the following reactions:



The equilibrium constants, considered as the dissociation constants of the sites  $\equiv\text{SOH}_2^+$  and  $\equiv\text{SOH}$  ( $K\alpha_1$  and  $K\alpha_2$ ) can be written:

$$K\alpha_1 = \frac{X_{\text{SOH}} \times a_{\text{H}^+}}{X_{\text{SOH}_2^+}} \quad (2)$$

$$K\alpha_2 = \frac{X_{\text{SO}^-} \times a_{\text{H}^+}}{X_{\text{SOH}}} \quad (3)$$

where  $X_i$  denotes the molar fraction of surface species and  $a_{\text{H}^+}$  is the aqueous proton activity. The surface density of any complex,  $\theta_i$  is defined as the number of complexes per unit surface area ( $\mu\text{mol}/\text{m}^2$ ). If  $\theta_M$  is the total surface density site, the surface density of any species can be obtained by:

$$\text{For protonation site: } \theta_I = \theta_{\equiv\text{SOH}_2^+} = X_{\equiv\text{SOH}_2^+} \times \theta_M$$

$$\text{For deprotonation site: } \theta_{II} = \theta_{\equiv\text{SO}^-} = X_{\equiv\text{SO}^-} \times \theta_M$$

Consequently, after rearranging (Eqs. 2 and 3), the values of  $K\alpha_1$  and  $K\alpha_2$  were obtained:

$$K\alpha_1 = \frac{a_{\text{H}^+}}{\theta_I \times \theta_M^{-1}} - a_{\text{H}^+}$$

$$K\alpha_2 = \frac{\theta_{II} \times \theta_M^{-1} \times a_{\text{H}^+}}{\left(1 - \frac{\theta_{II}}{\theta_M}\right)}$$

The surface site density was estimated by fitting the sections of the potentiometric titration curves for the two samples Na-EP and Zn-EP using a nonlinear least-square regression analysis (Fig. 5). Moreover, this regression provides the constants  $K\alpha_1$  and  $K\alpha_2$  for each reaction. The main results are summarized in Table 3 for mineral clays Na-EP and Zn-EP.

### 3.2.4. Modelling with ProtoFit

Modelling of the acid-base properties of the Na-EP and Zn-EP samples used the software ProtoFit [28] and considered the Non-Electrostatic Model (NEM) in order to determine the dissociation constants, and therefore the point of zero charge (PZC). The results are shown in Fig. 6 in which the curve represent the charge quantity  $Q^* = dQ_{\text{ads}}/dpH$  where  $Q_{\text{ads}}$  is the adsorbed proton variation per unit mass of adsorbent obtained by polynomial regression of the experimental values. The model was applied to both samples with 0.5 M ionic strength and 298 K.

The acid-base properties of both EP-Na and EP-Zn clays were described by two distinct surface sites. Fitting to the experimental data is good for the pH range of 4 to 10, but beyond this limit the fitting curve diverges from the experimental points. This is most probably due to dissolution processes that occur at these extreme pH values that interfere in the simple protonation/deprotonation reactions. Therefore, the surface sites undergo protonation/deprotonation on the pH domain of 4 to 10 only.

The values of the dissociation constants are extracted from the charge quantity curves (Fig. 6) while the PZC is computed from charge density curves (Fig. 7) and the results are given in Table 4. They are both shown to be very consistent with similar PZC, the difference being due to the different value for the  $pK\alpha_2$ . The modelled values are within the range obtained for the Na-EP with the previous procedure while for Zn-EP they are overestimated in relation to that same procedure.

### 3.2.5. Site distribution

In order to determine the site distribution for this system we used the PHREEQC code [29] feeding the chemical equilibrium model with the surface dissociation constants as obtained from ProtoFit and with the NEM. The results obtained are presented in the Fig. 8, where the surface dissociation constants have been directly taken from the graphic representation of species distribution. These results are shown in Table 5. The results again are in agreement with the ProtoFit model for the Na-EP sample, but

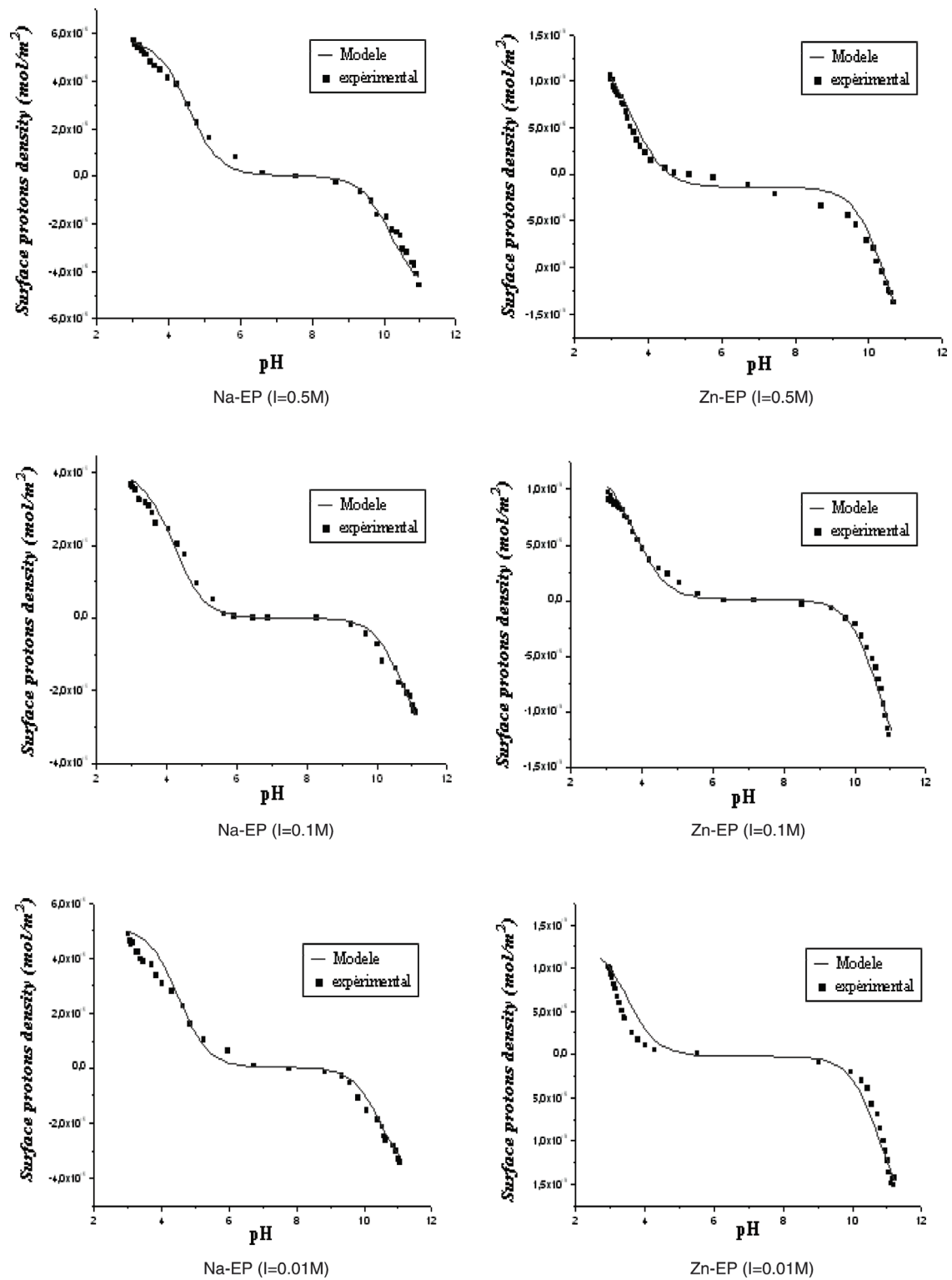


Fig. 5. Modeling of experimental acid-base titration of Na-EP and Zn-EP at various ionic strengths according to the NEM assuming a two site-two  $pK_a$  surface model.

Table 3

Surface site densities  $\theta$  ( $\mu\text{mol}\cdot\text{m}^{-2}$ ) and calculated equilibrium constants for protonation and deprotonation surface reactions for Na-EP and Zn-EP (subscripts “I” and “II” correspond to protonation and deprotonation reactions. Equilibrium constants are defined as surface dissociation constants, using pk scale.)

Sample	Na-EP			Zn-EP		
	0.5 M	0.1 M	0.01 M	0.5 M	0.1 M	0.01 M
Ionic strength						
$\theta_I$	5.96	5.25	3.80	15	12.3	13
$\theta_{II}$	4.24	3.63	2.74	10.2	11.2	20
$\theta_M$	10.2	8.88	6.54	25.2	23.5	33
$\text{pk}\alpha_1$	4.16	4.22	4.24	3.83	3.57	3.16
$\text{pk}\alpha_2$	10.24	10.28	10.42	10.20	9.41	10.54

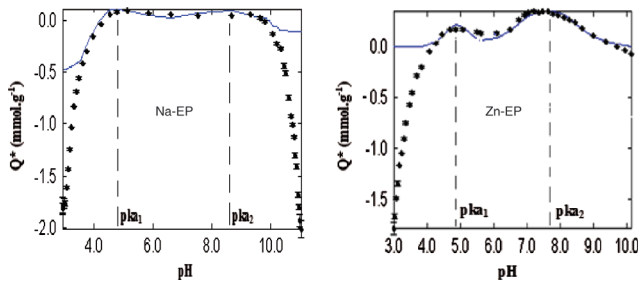


Fig. 6. Charge amount vs. pH, obtained by ProtoFit modelling.

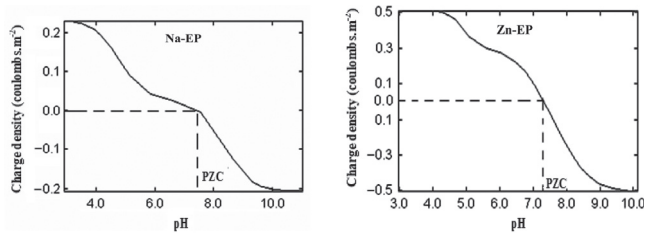


Fig. 7. Charge Density vs. pH, obtained by ProtoFit modelling.

differ for the Zn-EP with respect to the PZC. As in the previous case it is precisely in the range of basic pH that one often encounters discrepancies on the  $\text{pk}\alpha_2$  determination. Nevertheless, all methods provide a range of PZC which, taken as a whole, may provide a good average description of the acid-base properties of the Na-EP and Zn-EP clays.

In summary, all the values of the point of zero proton charge PZC and the acidic constants  $\text{pk}\alpha$  obtained by different methods are synthesised in Table 6, and one may note that the  $\text{pk}\alpha_1$  values are in good agreement between all methods, while they differ notably in relation to the  $\text{pk}\alpha_2$  value, and this is also the major source of discrepancies between all methods for the PZC. However the

Table 4

Constant acidities and PZC values of Na-EP and Zn-EP samples estimated by ProtoFit model at  $I = 0.5 \text{ M}$

Sample	Na-EP	Zn-EP
$\text{pk}\alpha_1$	4.8	4.8
$\text{pk}\alpha_2$	8.4	7.8
PZC	7.49	7.34

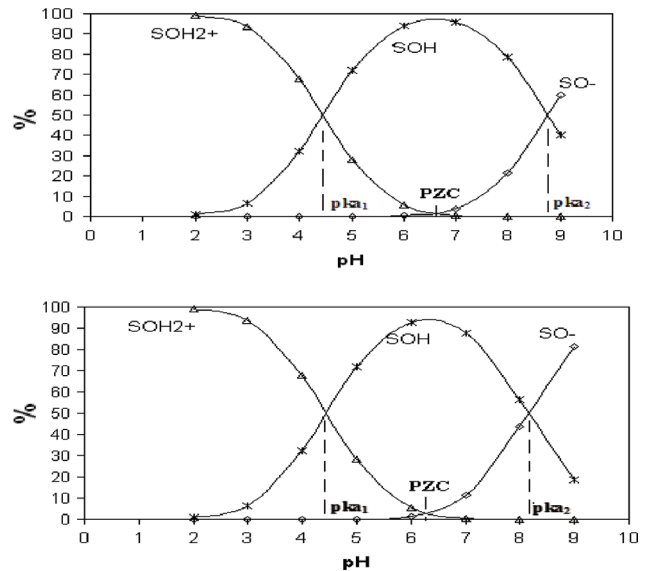


Fig. 8. Percentage Evolution of surface space of Na-EP and Zn-EP samples clay.

Table 5

Acidities constant and PZC values of Na-EP and Zn-EP, esteemed by PHREEQC at  $I = 0.5 \text{ M}$

Sample	EP-Na	EP-Zn
$\text{pk}\alpha_1$	4.42	4.40
$\text{pk}\alpha_2$	8.79	8.20
PZC	6.60	6.24

range of values is much less significant, with the Na-EP clay having a PZC between 6.40 and 7.50, and the Zn-EP clay having a PZC between 6.10 and 7.35. As a mean surface property the range of these values is not much significant and provides a good insight for the behaviour of the mineral surfaces during the adsorption processes.

### 3.3. Adsorption isotherms

Fig. 9 contains the constant-pH adsorption isotherms of ions  $\text{Zn}^{+2}$  on purified smectite Na-EP at 0.5 M and 0.01 M NaCl concentration, respectively. Each isotherm

Table 6  
Acidity constants and PZC values of Na-EP and Zn-EP samples at  $I = 0.5$  M

	Na-EP			Zn-EP		
	$\text{p}K_{\alpha_1}$	$\text{p}K_{\alpha_2}$	PZC	$\text{p}K_{\alpha_1}$	$\text{p}K_{\alpha_2}$	PZC
Graphic determination	4.16	10.24	7.20	3.83	10.20	7.02
Mass titration	****	****	6.39	****	****	6.08
Modelling by ProtoFit	4.80	8.40	7.49	4.80	7.80	7.34
Modelling by PHREEQC	4.42	8.79	6.60	4.40	8.20	6.24

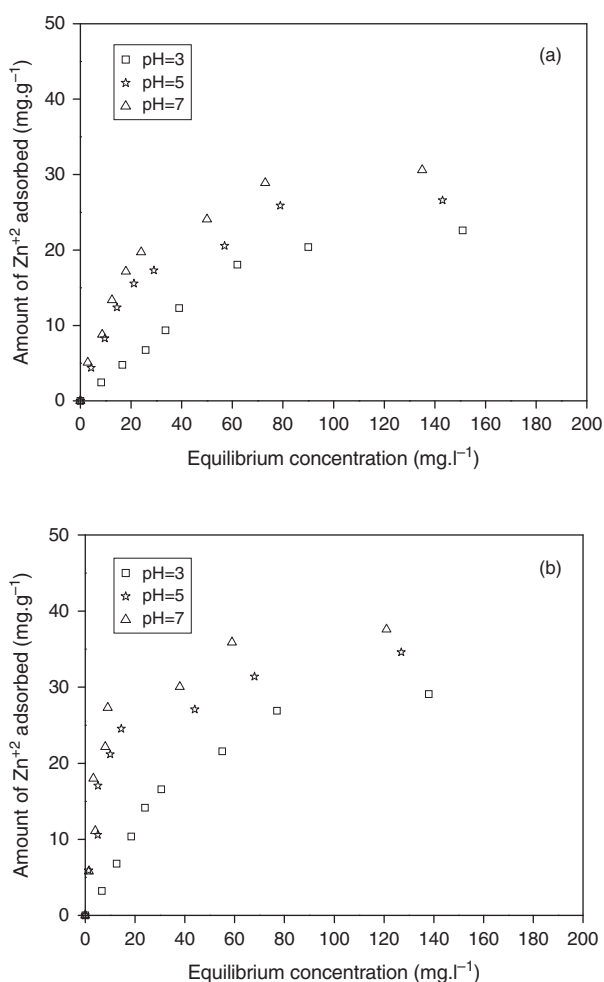


Fig. 9. adsorption isotherms of Zn<sup>2+</sup> on EP-Na at different pH (a) at  $I = 0.5$  M and (b) at  $I = 0.01$  M.

represents the variation of amount of Zn adsorbed on Na-EP,  $Q_{ad}$ , expressed in ( $\text{mg}\cdot\text{g}^{-1}$ ), against the Zn equilibrium concentration  $C_{\text{eq}}$ , expressed in ( $\text{mg}\cdot\text{l}^{-1}$ ). The amount  $Q_{ad}$  can be given by:

$$Q_{ad} (\text{mg}\cdot\text{g}^{-1}) = \frac{(C_0 - C_{\text{eq}}) \times V_s}{m} \quad (4)$$

where  $C_0$ ,  $C_{\text{eq}}$ ,  $V_s$  and  $m$  are the initial metal ion concentration ( $\text{mg}\cdot\text{l}^{-1}$ ), equilibrium metal ion concentration ( $\text{mg}\cdot\text{l}^{-1}$ ), the suspension volume (ml) and the amount of mineral solid (mg), respectively.

The initial slope and the amount of ions Zn<sup>2+</sup> adsorbed increase according to Giles classification [30], the adsorption isotherms at different pH and ionic strength were L-type, characterized by a decreasing slope as concentration increases since vacant adsorption sites decrease as the adsorbent becomes covered. This suggests that the clay particles have a high affinity for the metal ions at low concentration and a decreasing affinity as the adsorbed metal concentration approaches the maximum adsorption capacity of the clay [31].

### 3.3.1. Effect of pH

Fig. 9 illustrates the relationship between the amount adsorbed and pH for different initial concentration of Zn<sup>2+</sup> in 0.5 M and 0.01 M NaCl. As it can be seen from the Fig, the adsorption capacity of Na-EP increases when the initial pH of the solution was increased from 3 to 7. The maximum amount of adsorbed Zn<sup>2+</sup> occurred with the initial solution pH of 7 and the lower amount adsorbed were obtained at pH = 3. In addition, the adsorption of Zn on Na-EP is strongly dependent on pH and increases with increasing pH. These results are in agreement with other studies performed with smectite [6,32]. This could be due to the increase in competition for adsorption sites by H<sup>+</sup> [1,14] and dissolution of Al<sup>3+</sup> ions from the aluminosilicates layers for pH = 3 [4]. In addition, at lower pH (below  $\text{pH}_{\text{PZC}}$ ), as more of the surface sites are positively charged, adsorption of Zn(II) ion is inhibited by electrostatic repulsion [33].

Table 7  
Langmuir and Freundlich isotherms parameters

Ionic strength	pH	0.5 M			0.01 M		
		3	5	7	3	5	7
Langmuir parameters	$Q_{\text{max}}$	89.28	34.84	29.76	89.28	34.84	29.76
	K	0.003	0.03	0.07	0.01	0.15	0.10
	$R^2$	0.99	0.99	0.96	0.99	0.99	0.96
Freundlich parameters	$K_f$	0.50	2.70	3.53	1.11	7.17	8.21
	$n$	0.81	0.50	0.48	0.73	0.36	0.36
	$R^2$	0.95	0.91	0.93	0.91	0.85	0.76

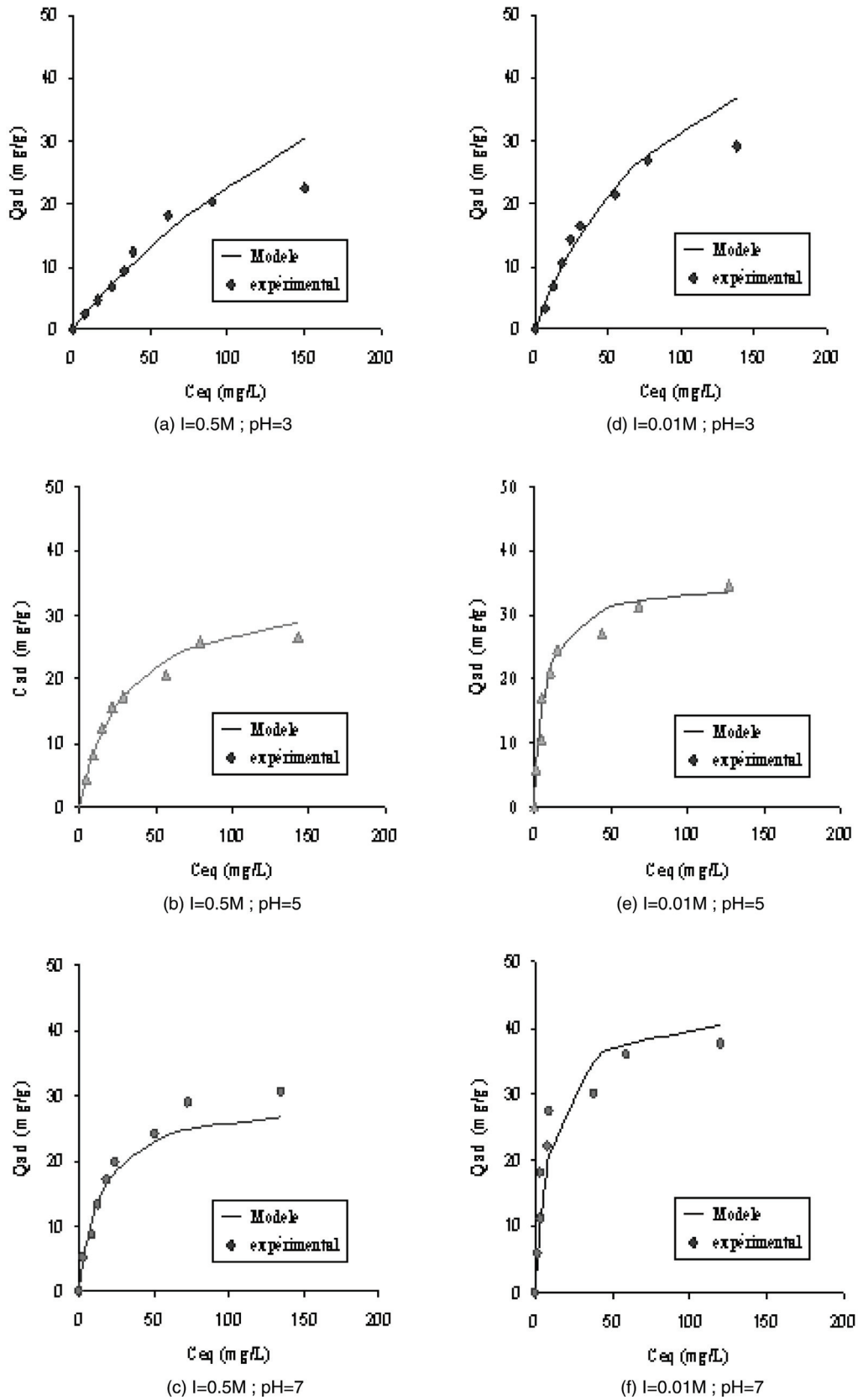


Fig. 10. Comparison of the experimental results with  $Q_{ad}$  values obtained by Langmuir models.

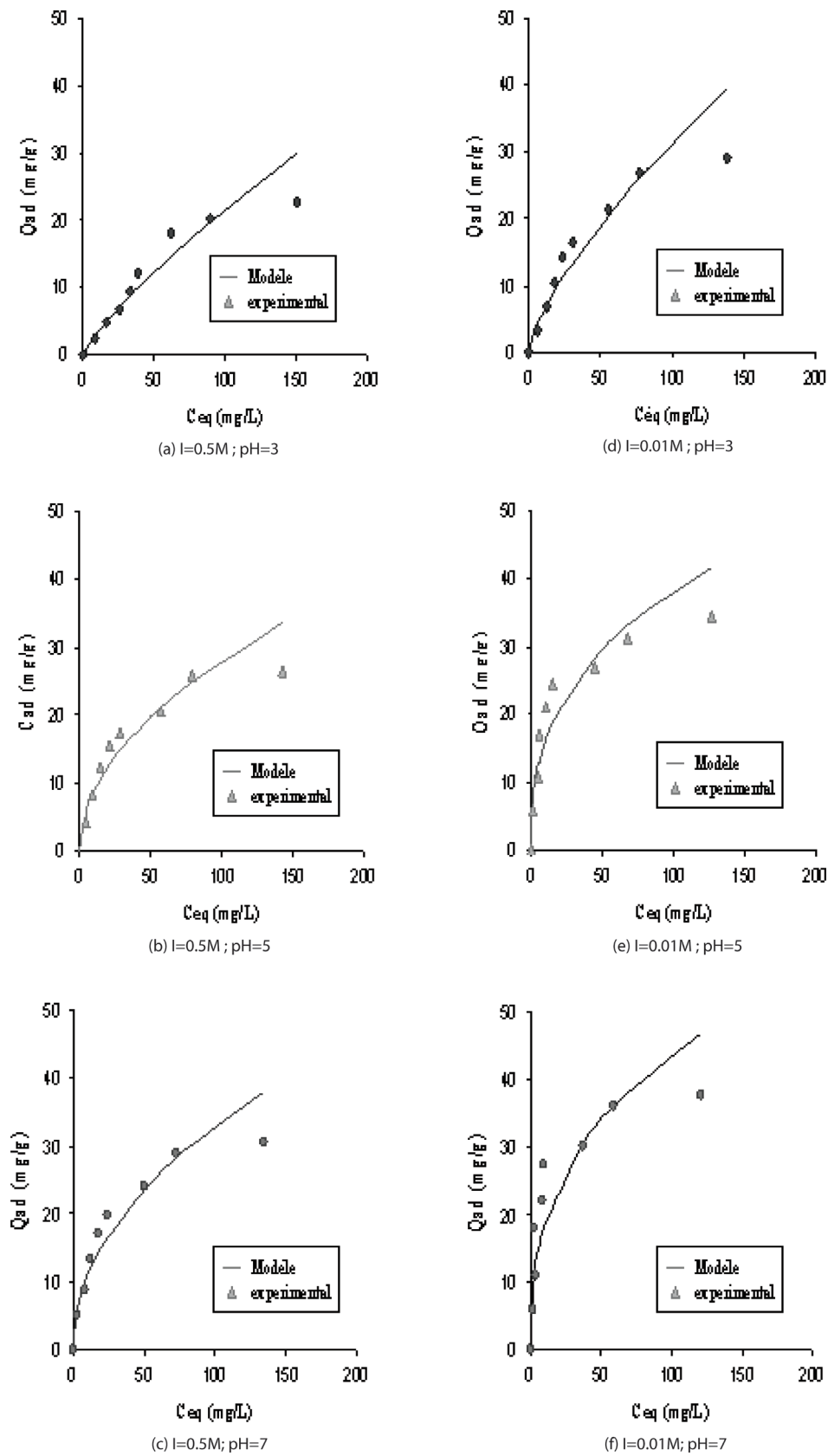


Fig. 11. Comparison of the experimental results with  $Q_{ad}$  values obtained by Freundlich isotherms.

The basic mechanism that governs the adsorption characteristics of Na-smectite at the pH range under study is adsorption and ion exchange as the dominating process [34]. At these pH values, exchangeable ions present at the exchangeable sites, i.e.,  $\text{Na}^+$ ,  $\text{K}^+$ ,  $\text{Ca}^{2+}$  and  $\text{Mg}^{2+}$  are exchanged for  $\text{Zn}^{2+}$  ions in the aqueous solution.

### 3.3.2. Effect of ionic strength

The effect of ionic strength on the adsorption of Zn(II) by EP-Na was examined only at 0.5 M and 0.01 M NaCl concentration. As it can be seen from the plots of the adsorption vs. concentration of  $\text{Zn}^{2+}$  remaining in solution at NaCl concentrations 0.5 M and 0.01 M at pH = 3 (Fig. 9), the amount of Zn adsorbed decreased when the concentration of NaCl in solution increases from 0.01 M to 0.5 M. Generally, increasing the ionic strength of the solution would result in reduced sorption of metals in a soil system; thus, there exists an inverse relationship between ionic strength and the distribution coefficient  $K_d$  [12]. Brigatti [37] and Auboiroux [7] found that increasing the ionic strength of a  $\text{CaCl}_2$  solution significantly decreases adsorption of Zn from the soil because of competition between Ca and Zn for the adsorption sites. Results of our experiment showed that the adsorption of Zn actually decreased with increasing ionic strength of NaCl in the solution; this is a consequence of the enhancement of the competition of  $\text{Na}^+$  with Zn(II) by the sorption sites of smectite.

### 3.3.3. Modelling adsorption isotherms

Adsorption isotherms of Na-EP for zinc ions were expressed mathematically in terms of the Langmuir and Freundlich models. The obtained experimental data are commonly well fitted by the Langmuir (Eq. 5) and Freundlich (Eq. 6) models:

$$Q_{ad} = \frac{Q_M K C_{\acute{e}q}}{1 + K C_{\acute{e}q}} \quad (5)$$

$$Q_{ad} = K_f C_{\acute{e}q}^n \quad (6)$$

were  $K$ ,  $K_f$  and  $n$  are the constant for Langmuir and Freundlich models, respectively and  $C_{\acute{e}q}$  is the equilibrium concentration. The values of the regression coefficients  $R^2$  and parameters obtained from both models are given in Table 7.

The adjustment of adsorption data to the different empirical models show that pH-constant isotherms of Na-EP adjust better to the Langmuir model. This model effectively describes the sorption with all  $R^2$  values > 0.96. The Table indicates also that the Freundlich model has a limited application for Zn(II) sorption

at ( $I = 0.01$  M; pH = 5 and 7) with regression coefficients,  $R^2 = 0.85$  and  $R^2 = 0.76$  respectively. Moreover, the comparison of the experimental values with the values of  $Q_{ad}$  obtained by both models is shown Figs. 10 and 11. As it is seen in the figure Langmuir isotherms usually fit the experimental data better.

## 4. Conclusion

The surface charge characterization of the EP-Na and EP-Zn clays were determined by the mass titration and potentiometric titration methods. These methods allowed us to obtain the acid-base properties of the clay minerals surface, both the surface dissociation constants and the point of zero proton charge (PZC). Both clay surfaces are described by protonation and deprotonation reactions over two surface sites. The effect of ionic strength allowed us to note that: i) the values of the charge density decreased in the acidic sites and increased in the basic sites with decreasing ionic strength; ii) ionic strength had a slightly effect on the PZC apart for some slight deviations. Surface dissociation constants were determined by nonlinear least squares to a two surface site model (average over all ionic strengths) and also optimised with the ProtoFit and estimated with PHREEQC models.

The adsorptive behaviour of  $\text{Zn}^{2+}$  ions was strongly dependent on the pH solution and the ionic strength with maximum Zn removal occurring at pH 7 and 0.01 M NaCl ionic strength with cation exchange as the basic mechanism. The adsorption isotherms were described by means of Freundlich and Langmuir models. The last model is better to represent the adsorption process.

## References

- [1] M. Fonseca, M. Oliveira and L. Araka, Removal of cadmium, zinc, manganese and chromium cations from aqueous solution by a clay mineral, *J. Hazard. Mater.*, 137 (2006) 288–292.
- [2] O. Abollino, M. Acetob, M. Malandrino, C. Sarzaninia and E. Mentastia Adsorption of heavy metals on Na-montmorillonite: Effect of pH and organic substances, *Water Res.*, 37 (2003) 1619–1627.
- [3] S. Dahiya, A.V. Shanwal and A.G. Hegde, Studies on the sorption and desorption characteristics of Zn(II) on the surface soils of nuclear power plant sites in India using a radiotracer technique, *Chemosphere*, 60 (2005) 1253–1261.
- [4] A. Kaya and H. Oren, Adsorption of zinc from aqueous solutions to bentonite, *J. Hazard. Mater.*, 125 (2005) 183–189.
- [5] D. Singh, G. McLaren and C. Cameron, Zinc sorption–desorption by soils: Effect of concentration and length of contact period, *Geoderma*, 137 (2006) 117–125.
- [6] A.M. Kraepiel, K. Keller and F.M.M. Morel, A model for metal adsorption on montmorillonite, *J. Colloid Interf. Sci.*, 210 (1999) 43–54.
- [7] M. Auboiroux, P. Baillif, J. Touray and F. Bergaya, Fixation of  $\text{Zn}^{2+}$  and  $\text{Pb}^{2+}$  by a Ca-montmorillonite in brines and dilute solutions: Preliminary results, *Appl. Clay Sci.*, 11 (1996) 117–126.
- [8] B. Cothenbach, R. Krebs, G. Furrer, S.K. Gupta and R. Schulin, Immobilization of cadmium and zinc in soil by Al-montmorillonite and gravel sludge, *Soil Sci.*, 49 (1998) 141–148.

- [9] B. Baeyens and M. Bradbury, A mechanistic description of Ni and Zn sorption on Na-montmorillonite Part I: Titration and sorption measurements, *J. Contam. Hydrol.*, 27 (1997) 199–222.
- [10] J. Ikhsan, J. Wells, B. Johnson and M. Angove, Surface complexation modeling of the sorption of Zn(II) by montmorillonite, *Colloid. Surfaces*, 252 (2005) 33–41.
- [11] T. Vengris, R. Binkiene and A. Sveikanskaite, Nickel, copper and zinc removal from water by a modified clay sorbent, *Appl. Clay Sci.*, 18 (2001) 183–190.
- [12] D. Egrani, A. Baker and J. Andrews, Copper and zinc removal from aqueous solution by mixed mineral systems Part II. The role of solution composition and aging, *J. Colloid Interf. Sci.*, 291 (2005) 326–333.
- [13] T.D. Tsai and P.A. Vesilind, Zinc adsorption by lime-treated montmorillonite clay, *J. Environ. Sci. Heal., Part A*, 34 (1999) 103–124.
- [14] E. Alvarez-Ayuso and A. Garcia-Sanchez, Removal of heavy metals from waste waters by natural and Na-exchanged bentonites, *Clay Clay Miner.*, 51 (2003) 475–480.
- [15] M. Bradbury and B. Baeyens, A mechanistic description of Ni and Zn sorption on Na-montmorillonite Part II: modelling, *J. Contam. Hydrol.*, 27 (1997) 223–248.
- [16] M. Bradbury, and B. Baeyens, Modelling the sorption of Mn(II), Co(II), Ni(II), Zn(II), Cd(II), Eu(III), Am(III), Sn(IV), Th(IV), Np(V) and U(VI) on montmorillonite: Linear free energy relationships and estimates of surface binding constants for some selected heavy metals and actinides, *Geochim. Cosmochim. Ac.*, 69 (2005) 875–892.
- [17] L.I. Vico, Acid-base behaviour and Cu<sup>2+</sup> and Zn<sup>2+</sup> complexation properties of the sepiolite/water interface, *Chem. Geol.*, 198 (2003) 213–222.
- [18] H. Van Olphen, 1963. An introduction to clay colloid chemistry, Interscience publishers, New York, London (1963).
- [19] F. Bergaya and M. Vayer, CEC of clays: Measurement by adsorption of a copper ethylenediamine complex, *Appl. Clay Sci.*, 12 (1997) 275–280.
- [20] J. Noh and J.A. Schwarz, Estimation of the point of zero charge of simple oxides by mass titration, *J. Colloid Inter. Sci.*, 130 (1989) 157–163.
- [21] A. Kriaa, N. Hamdi and E. Srasra, Surface properties and modeling potentiometric titration of aqueous illite suspensions, *Surface Engineering and Applied Electrochemistry*, 44 (3) (2008), 217–229.
- [22] B. Caglar, B. Afsin, A. Tabak and E. Eren, Characterization of the cation-exchanged bentonites by XRPD, ATR, DTA/TG analyses and BET measurement. *Chem. Eng. J.*, 149 (2009) 242–248.
- [23] B.L. Schroth and G. Sposito, Surface charge properties of kaolinite, *Clays. Clay Miner.*, 45 (1997) 85–91.
- [24] F. Huertas, L. Chou and R. Wollast, Mechanism of kaolinite dissolution at room temperature and pressure: Part I. Surface speciation, *Geochim. Cosmochim. Ac.*, 62 (1998) 417–431.
- [25] A. Kriaa, N. Hamdi and E. Srasra, Acid–Base Chemistry of Montmorillonitic and Beidellitic-Montmorillonitic Smectite, *Russ. J. Electrochem.*, 43 (2007) 167–177.
- [26] E. Tombacz and M. Szekeres, Colloidal behaviour of aqueous montmorillonite suspensions: the specific role of pH in the presence of indifferent electrolytes, *Appl. Clay Sci.*, 27 (2004) 75–94.
- [27] M. Duc, F. Gaboriaud and F. Thomas, Sensitivity of the acid–base properties of clays to the methods of preparation and measurement 2. Evidence from continuous potentiometric titrations, *J. Colloid Interf. Sci.*, 289 (2005) 148–156.
- [28] G. Sposito, Surface reactions in natural aqueous colloidal systems, *Chimia*, 43 (1998) 169–176.
- [29] L. Weiping and H.S. Edward, Modeling potentiometric titration behavior of glauconite, *Geochim. Cosmochim.*, 60 (1996) 3363–3373.
- [30] B.F. Turner and J.B. Fein. Proffit: A program for determining surface protonation constants from titration data, *Computat. Geosci.*, 32, (2006) 1344–1356.
- [31] D.L. Parkhurst and C.A.J. Appelo, User's guide to PHREEQC (version 2) – a computer program for speciation, batch-reaction, one-dimensional transport, and inverse geochemical calculations. Water-Resources Investigations Report (1999) 99–4259.
- [32] C.H. Giles and D.A. Smith, A general treatment and classification of solute adsorption isotherm, *J. Colloid Interf. Sci.*, 47 (1974) 744–765.
- [33] E.F. Covelo, N. Alvarez, M.L. Andrade Couce, F.A. Vega and P. Marcet, Zn adsorption by different fractions of Galician soils, *J. Colloid. Interf. Sci.*, 280 (2004) 343–349.
- [34] A. Kaya and A.H. Oran. Adsorption of zinc from aqueous solution to bentonite, *Hazard. Mater.*, B125 (2005) 183–189.
- [35] M. Sarkar, A.R. Sarkar and Goswami, Mathematical modelling for the evaluation of zinc removal efficiency on clay sorbent, *J. Hazard. Mater.*, 14 (2007) 666–674.
- [36] A.G. Zhang, Y. Liu, Y. Xie, X. Yang, B. Hu, S. Ouyang, H. Liu, H. Wang, Zinc adsorption on Na-rectorite and effect of static magnetic field on the adsorption, *Appl. Clay Sci.* 29 (2005) 15–21.
- [37] M.F. Brigatti, F. Corradini, G.C. Franchini, S. Mazzoni, L. Medici and L. Poppi, Interaction between montmorillonite and pollutants from industrial waste-waters: exchange of Zn<sup>2+</sup> and Pb<sup>2+</sup> from aqueous solutions, *Appl. Clay Sci.*, 9 (1995) 383–395.